Pre-normative REsearch for Safe use of Liquid Hydrogen (PRESLHY)

Project Deliverable

Summary of experiment series E4.3 (Electrostatic Ignition) results

Deliverable Number:	4.6
Work Package:	4
Version:	1.0
Author(s), Institution(s):	Kieran Lyons, HSE; Phillip Hooker, HSE
Submission Date:	04/2020
Due Date:	01/2020
Report Classification:	Confidential

FUEL CELLS AND HYDROGEN JOINT UNDERTAKING

History		
Nr.	Date	Changes/Author
0.1	03/02/2020	First draft.
1.0	06/04/2020	First issue.

Approvals			
Version	Name	Organisation	Date

Acknowledgements

This project has received funding from the Fuel Cells and Hydrogen 2 Joint Undertaking under the European Union's Horizon 2020 research and innovation programme under grant agreement No 779613. The HSE work programme acknowledges funding from its sponsors Shell, Lloyd's and Equinor and instrumentation provided by NREL and Dräger

Disclaimer

The data management in the PRESLHY project follows the principle of data management, which shall make data Findable, Accessible, Interoperable and Re-usable (FAIR). The plan for FAIR data management as described in this document is based on the corresponding template for open research data management plan (DMP) of the European Research Council (ERC).

Despite the care that was taken while preparing this document the following disclaimer applies: The information in this document is provided as is and no guarantee or warranty is given that the information is fit for any particular purpose. The user thereof employs the information at his/her sole risk and liability.

The document reflects only the authors' views. The FCH JU and the European Union are not liable for any use that may be made of the information contained therein.

Key words

FAIR data management, pre-normative research, experimental data, accessibility, re-use, long-term data storage, research data repository, liquid hydrogen, accidental behaviour, release, ignition, combustion, electrostatic.

Publishable Short Summary

Work package four of the PRESLHY project focuses on ignition phenomena. This report summarises the experimental series E4.3, which focuses on the propensity for an electrostatic charge capable of igniting a hydrogen cloud to be generated during a release, or accidental spill scenario. Seven experiments measuring the electric field of a multiphase hydrogen jet were conducted at the HSE Science and Research Centre. Current measurements on an electrically isolated section of steel pipework were also taken during a total of 30 large scale releases.

The results from the plume measurements indicate that the multiphase hydrogen jet itself does not create a significant charge, but certain interactions with the air can cause intermittent spikes in field strength. In particular, air in the pipework being ejected and solidified air forming around the release point, breaking off and flowing downstream appear to be the cause of the electrical fields measured in these experiments. This effect could be larger with different initial conditions either at the nozzle or in the tanker.

The wall current measurements were more consistent, as the ability for LH_2 to induce a current on a section of electrically insulated pipework was clearly demonstrated. This charge is a complicated function of the phase of LH_2 in the pipework, the turbulence of the flow, and the resistance to ground of the section of the pipework. Frost formation on the outside of the pipework dynamically changed the resistance to ground throughout each trial, making interrogation of the results difficult.

The experiments show that electrostatic charges do pose a credible hazard when considering LH_2 facilities. The charging, however, does not form inside the hydrogen, but on the substances or objects that the hydrogen interacts with. For a fixed facility, maintaining continuity to earth, paying attention to objects in the potential path of a release, would limit the likelihood of electrostatic charging and therefore limit the hazard.

Table of Contents

1 Introduction

Work package four of the PRESLHY project focusses on ignition phenomena. The experimental programme has been designed to examine a number of credible LH_2 ignition scenarios. One such scenario is the propensity for LH_2 to cause electrostatic charging in leak or spillage scenarios, which may lead to ignitions. This report summarises the large-scale experiments carried out at the HSE Science and Research Centre investigating the possible modes of electrostatic charging present in LH_2 releases from steel pipework.

The experiments were designed to measure two distinct modes of charging: the charging due to charge separation near to the LH_2 / pipe interface (monitored via the wall current from an electrically isolated section of pipework) and the charged cloud generated by a jet of hydrogen, which may be liquid, gaseous or two-phase.

The wall current measurements were made using an electrometer connected to an electrically isolated section of pipework prior to the release point. As well as five of the seven electrostatic trials, wall current measurements were also taken during the 25 rainout experiments, summarised in deliverable D3.6 [1].

In order to measure the charged cloud formed by the hydrogen jet, a series of seven experiments were conducted whereby LH_2 was released, with various initial conditions, through the path of a field meter. A Faraday cage was also used on some of the trials to better enable characterisation of the electric field geometry.

For a full assessment of the electrostatic measurement methods that were considered and the rational for adopting those that were used, see PRESLHY deliverable, D4.1 [2].

2 Theoretical considerations

This section contains a brief summary of the theoretical aspects of interest in this experimental campaign, the reasoning behind the selected measurement methods and a retrospective analysis of the predictions set out in D4.1.

2.1 Liquid charging as a result of flow along a pipe

As a liquid flows through a pipe it will become charged due to the interaction with the pipe wall. The liquid will charge as it progresses along the pipe until it reaches a maximum charge density (charge per unit volume). The charge density multiplied by the flow rate of the liquid results in a measurement of current (i.e. charge per second i.e. Amps), known as the streaming current. The degree of charging is dependent upon many variables. However, for insulating liquids, a summary of the work of several researchers (Cross 1987) [3] shows that the maximum streaming current carried by a turbulently flowing liquid would be defined by a function of the form:

$$I_\infty = K d^\alpha v^\beta \qquad \textit{(Eq. 1)}$$

Where I_∞ = streaming current after travelling an infinite distance along the pipe (A)

d = internal pipe diameter (m)

v = velocity of liquid in the pipe (m s^{-1})

α and β are constants approximately equal to 2

K = a constant equal to 4 µA s^2 m^{-4}

This function is known as the Schon equation.

As stated above, the degree of charging (and hence streaming current) increases as the liquid flows along the pipe, as illustrated in Figure 1.

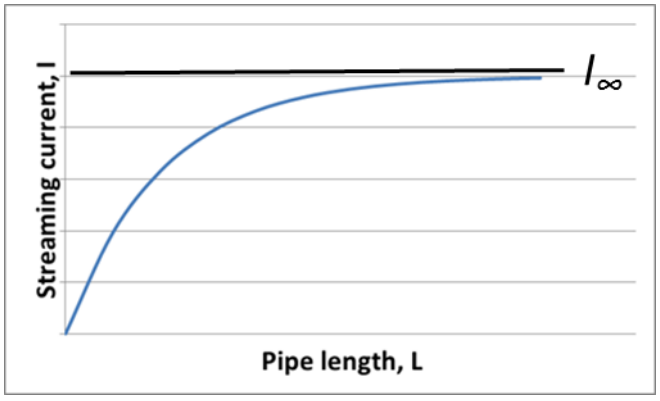

Figure 1: Plot of current against pipe length.

The streaming current at distance, L, along the pipe can be expressed as a proportion of the maximum streaming current, I_∞, using the relationship:

$$\boldsymbol{I_L = I_\infty(1 - e^{\left(-\frac{L}{v\tau}\right)})} \qquad \textit{(Eq. 2)}$$

Where: I_L = streaming current after travelling a distance, L, along the pipe (A)

I_∞ = streaming current after travelling an infinite distance along the pipe (A)

v = velocity of liquid in the pipe (m s^{-1})

L = distance along the pipe (m)

τ = relaxation time of the liquid (s), defined by Equation 3.

$$\boldsymbol{\tau = \varepsilon_0 \varepsilon_r \rho} \qquad \textit{(Eq. 3)}$$

Where: τ = relaxation time of the liquid (s)

ε_0 = permittivity of air (ca. 8.85 x 10^{-12} F m^{-1})

ε_r = relative permittivity of the liquid

ρ = resistivity of the liquid (Ω m)

Equation 2 can be re-arranged to calculate the length of pipe corresponding to a chosen fraction of the maximum current, i.e. I_L / I_∞:

$$\boldsymbol{L = -v\tau\, ln(1 - \frac{I_L}{I_\infty})} \qquad \textit{(Eq. 4)}$$

Previous analysis reported in deliverable D4.1 indicates that a pipe length far greater than that experimentally possible would be required to achieve half of the maximum streaming current, and for the proposed length of pipe/hose in the experimental system of ca. 35 m, the streaming current would be expected to peak at only tens of pA. In practice, this would be difficult to measure, especially in an open environment where stray currents due to impact charging from airborne dust etc. may be of a similar order of magnitude.

An attempt could be made to determine the streaming current by observing the voltage acquired by an isolated section of pipe and calculating the charge on the liquid within. However, due to the difficulties anticipated in achieving and maintaining a suitable level of electrical isolation for the section of pipe, as was born out in practice, this method was not adopted. Alternatively, measurements were made of the wall current, which is a measure of the rate of charge transfer to the pipe from the liquid during transit through it, as illustrated in Figure 2. While this does not give a measure of the streaming current, it does give an indication of how much charge transfer is taking place within the isolated pipe section. Wall current was measured from an isolated section of pipe, to earth, via an

electrometer with a very low input impedance, since this imposes a far lower burden on the degree of isolation required.

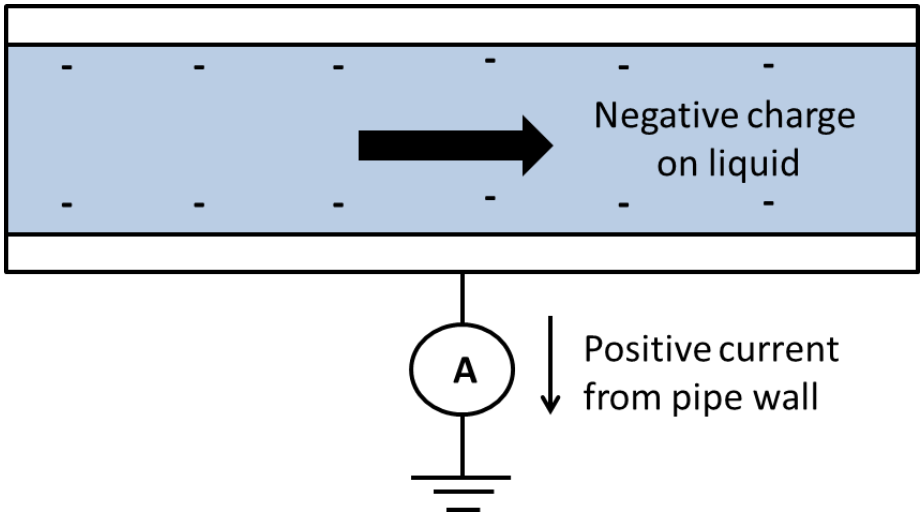

Figure 2: Measurement of wall current.

In the above analysis, it is assumed that the flow in the pipe is single phase, i.e. only liquid. The results indicate that two phase flow occurred in many cases, resulting in far higher currents than would be expected for single phase flow.

2.2 Charge

Charged clouds may form when LH_2 emerges from a leak (such as a hole in a pipe), and this may create an ignition hazard as the hydrogen mixes with the air to form a flammable mixture. The charged clouds could potentially consist of liquid hydrogen and liquefied or solidified water vapour (such as ice formed at the leak point subsequently breaking off) or condensed components of the air itself. Charged clouds may result in ignition by a number of mechanisms such as: inducing hazardous potentials on isolated conductors (for example, lumps of ice), promoting corona discharges even from earthed surfaces, or lightning-type discharges if the charged cloud is large enough.

The field produced by the cloud can be measured using an electric field meter.

A field meter placed facing the cloud (or jet) can be used to estimate the charge per unit length of the cloud as shown in Figure 3.

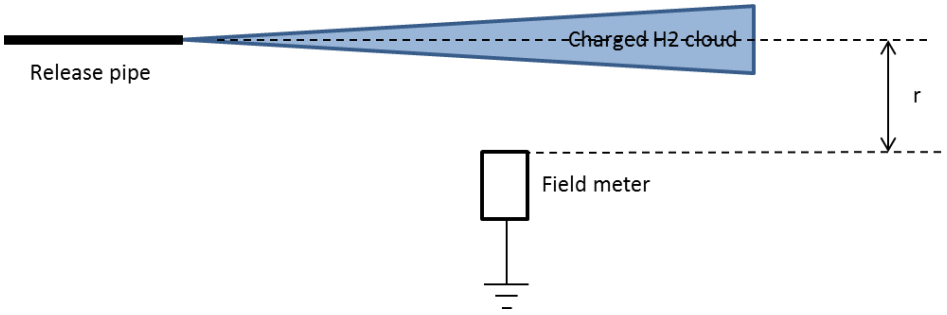

Figure 3: Diagram of electrostatic plume measurement.

The measured field can be analysed by assuming that the jet acts as a uniformly charged cylinder. Since the field measurement was made outside of the charged jet then, assuming the length is long compared to the radius, the field is estimated as:

$$\boldsymbol{E} = \frac{\boldsymbol{\lambda}}{\boldsymbol{2\pi\varepsilon_0\varepsilon_r r}} \qquad \textit{(Eq. 5)}$$

Where: E = electric field (V m^{-1})

λ- = charge per unit length (C m^{-1})

ε_0 = permittivity of free space (ca. 8.85 x 10^{-12} F m^{-1})

ε_r = relative permittivity of air

r = distance from axis of cylinder (m)

In order to establish a better defined geometry in which the electric field is present, an earthed cage can be placed around the jet, with the field meter "looking in" through a hole in the cage, as shown in Figure 4.

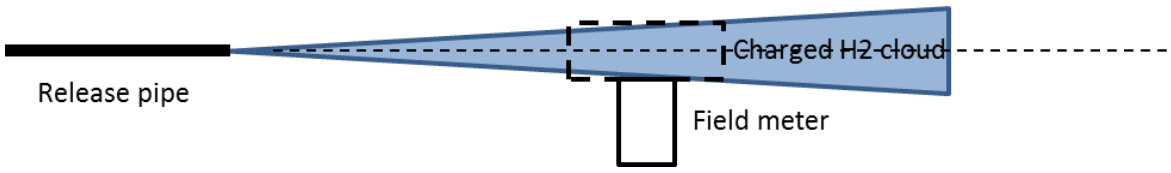

Figure 4: Diagram of electrostatic plume measurement using Faraday cage.

Assuming a uniform charge density within a cylindrical cage (a crude approximation) then the field, E, at the cage wall would be given by:

$$\boldsymbol{E} = \frac{\boldsymbol{\sigma R}}{\boldsymbol{2\varepsilon_0\varepsilon_r}} \qquad \textit{(Eq. 6)}$$

Where σ = charge density within the cloud (C m^{-3})

R = radius of the cage (m)

ε_0 = permittivity of air (ca. 8.85 x 10^{-12} F m^{-1})

ε_r = relative permittivity of the cloud, which will be approximately = 1

An advantage of this method is that the cage is earthed and therefore, it is not necessary to achieve an onerous level of electrical isolation.

It is not possible to predict the level of charging that would occur, especially for such a complex process as would occur with the LH_2 releases. However, initial results from KIT [4], completed as a part of the PRESLHY project, enabled the field meter to be set at a suitable range and distance to achieve a reasonable response from the field meter.

3 Method

This section contains a brief description of the test facility, data acquisition and experiment procedure. The details needed to fully interpret the results are found in Appendix A in the form of figures and tables. The dimensions of the equipment, locations of instrumentation and the format of the output data are included.

3.1 Facility & instrumentation

The experiments were conducted using the LH_2 release facility, which was located on a 32 m diameter concrete pad at the Frith Valley site at the HSE Science and Research Centre in Buxton. The experiments had three main components: the release station, the LH_2 tanker and the instrumentation. Due to the focus of these experiments, the layout downstream of the release point is not described in detail in this report.

3.1.1 Release station

The release station encompassed the pipework and valves required to operate the system remotely. For these tests this consisted of an electrically isolated pipe section, a valve section and a flexible hose. The pipework and a nominal bore of 25.4 mm. A 20 m vacuum insulated hose connected the release station to the tanker and a mixture of foam, aluminium tape and insulation tape covered the remaining parts. Figure 5 shows the release station after a trial.

Figure 5: Photo of release station.

The distances from each sensor in the pipework to the release point and dimensions of the pipe sections, including the approximate R values for the insulation, are available in tables A1 and A2 respectively in Appendix A.

3.1.2 Tanker

The LH_2 was supplied by Air Liquide in a vacuum insulated tanker, which could hold up to 2.5 tonnes. Control of the pressure and conditioning of the LH_2 inside the tanker was achieved through venting the ullage of hydrogen gas to lower the pressure, or allowing LH_2 into a heat exchanger underneath the tanker to raise the pressure. A 12 barg bursting disk protected the tanker against over pressurisation.

The tanker was connected to the release pipework, 3 m vent stack and valve control system. Figure 6 shows the tanker connected to the vent stack. The gas cylinders shown in the photo were used to purge the pipework of air prior to each release.

Figure 6: Photo of tanker, vent stack, and purging station.

3.1.3 Instrumentation

The instrumentation falls into three categories: electrostatic measurement, LH_2 flow characterisation and ambient condition monitoring.

The wall current was measured using a Keithley 6514 electrometer. The electrometer was connected to the 0.5 m section of electrically isolated pipework with a 20 m 50 Ω coaxial cable. Figure 7 shows the section of electrically isolated pipework and the connection to the electrometer. Figure 8 shows the method of electrical isolation, which includes PTFE

gaskets and bolt sleeves, phenolic insulation and a Mylar wrap. In order to interpret the output from the electrometer, resistance to ground measurements were taken with a RT-1000 resistance meter periodically during the test days. Two field meters were used throughout the experimental series. The IDB Systems ID107HS static field meter was mounted in line with the stream of the jet as shown in Figures 9 and 10. The second field meter, the IDB Systems rugged field meter ID-939R, was used in conjunction with a Faraday pail. This setup is shown in Figure 11.

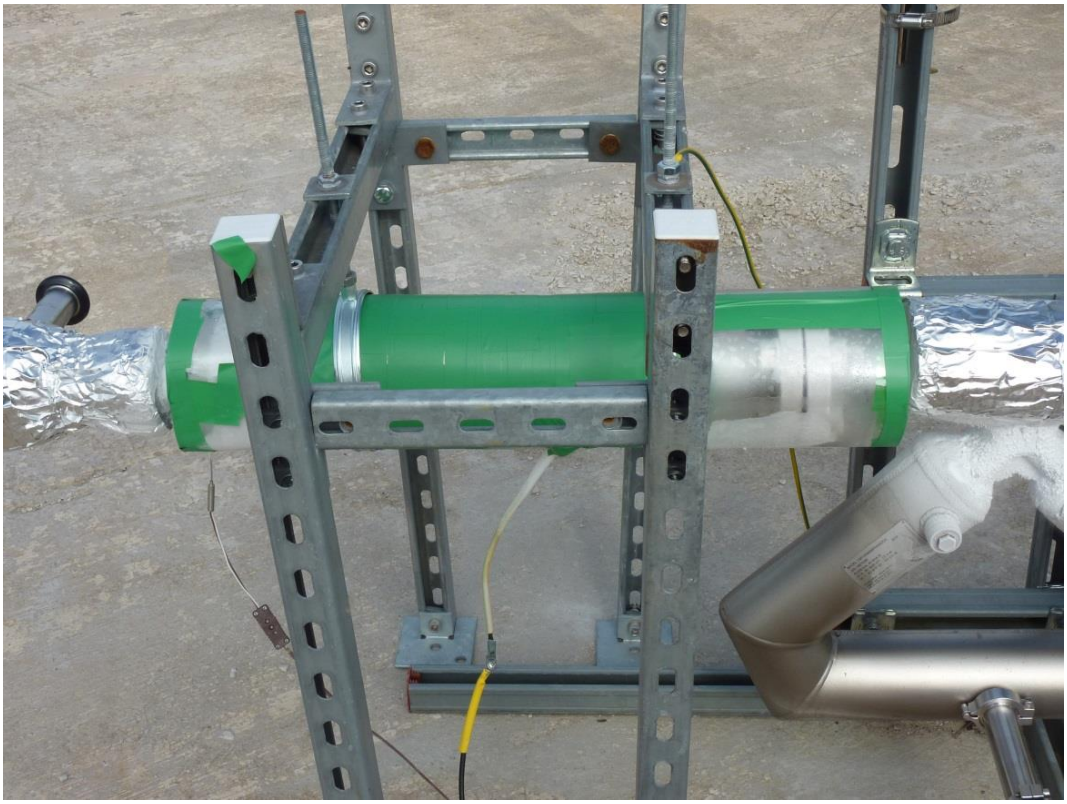

Figure 7: Photograph of the electrically isolated pipework section.

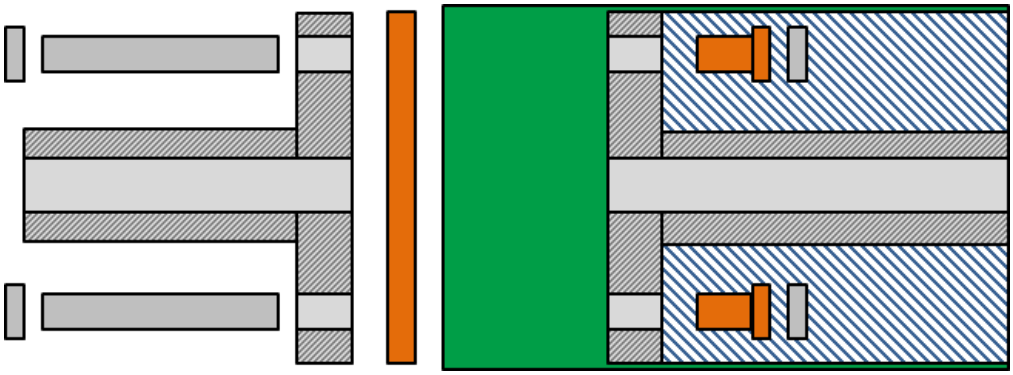

Figure 8: Diagram of an electrically isolated joint.

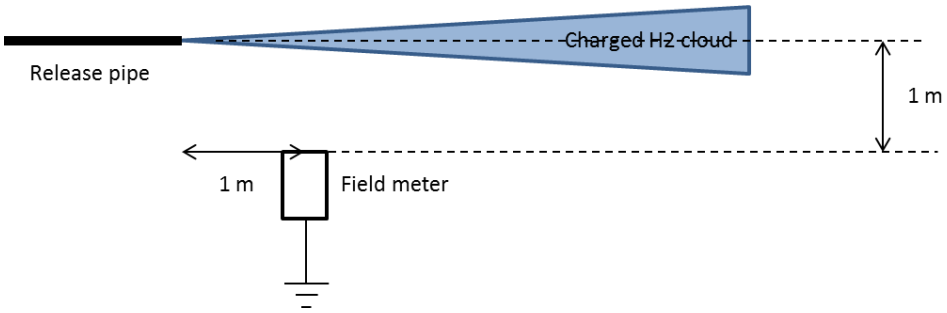

Figure 9: Sketch of the field meter layout 1.

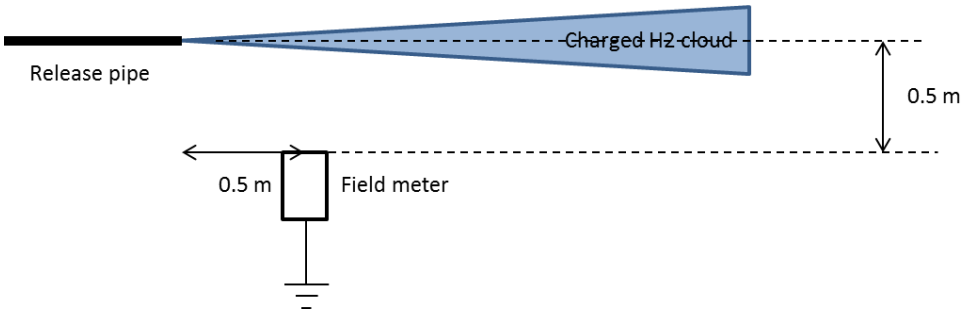

Figure 10: Sketch of the field meter layout 2.

Figure 11: Photograph of the field meter and Faraday cage setup.

In order to characterise the outflow properties of the LH_2, the release station included instrumentation consisting of two 10 bar Wika IS-3 pressure transducers, four 1.5 mm mineral insulated type T thermocouples and a Micro Motion Elite CFM100M coriolis mass flow meter with an Elite 5700 transmitter. The mass flow meter was modified by the manufacturer to help facilitate operation at temperatures below 70 K. The instrumentation on the tanker was not logged, but the pressure was recorded for each trial from the dial gauge on the tanker. One type T thermocouple was installed at the exit of the vent stack. Ambient conditions, including the relative humidity, were measured using two systems: a Skye SKH-2053 temperature and humidity probe mounted alongside a WindSonic ultrasonic anemometer on a 3 m high stand on the downwind edge of the concrete pad approximately 20 m from the release point; and a PCE-FWS-20 weather station was positioned locally to the release station at 1.5 m height.

3.2 Data acquisition

Various acquisition systems were used to collect the data from the instruments. The primary system not only logged, but also controlled the remotely operated valves. Each logging PC was networked and therefore shared a common time-base. Table A4 in Appendix A contains the channel headings and units that can be used to interpret the output of the data acquisition systems.

The primary method of acquisition and valve control was running on a dedicated PC with NI Flexlogger. Various National Instruments chassis and logging cards were used to collect data from the range of sensors. The wall current was logged through this system on all trials carried out through the three work packages. Each thermocouple and pressure transducer was logged through this system, as was the far-field weather station, which recorded humidity, wind speed and wind direction. The mass flow meter was also connected to the primary acquisition system. Logging was enabled before each test at a rate of 1 Hz.

The rugged field meter was connected directly to a PC running a bespoke logging system created by the manufacturer. This was in turn controlled via a remote connection.

The average weather conditions at the release point were logged once per 5 minutes on a separate system. The local weather station on the release point logged for the duration of each test day.

3.3 Estimate of measurement errors

The accuracy of the sensors used in the experiment are summarised below in Table 1. The information is taken from the respective manuals for the equipment. The inherent variability in conducting experiments outdoors needs to be taken into consideration when interpreting the results. While the electrometer was calibrated, the -2 to 2 V output that was logged in the data acquisition software was not. A pre-test check using another calibrated electrometer inputting a known current into the pipework indicated the correct output, although the uncertainties are somewhat higher than quoted on the specification and not fully quantified. However, these experiments were to investigate the order of magnitude of charging rather than to obtain precise values, in which case the uncertainties were acceptable.

Table 1: Sensor accuracies.

Sensor	Manufacturer	Model	Range	Accuracy
Rugged field meter	IDB systems	ID-939R	4 decade ranges from $\pm 10^2$ V/m to $\pm 10^5$ V/m	±5% range max
Static field meter	IDB systems	ID107HS	4 decade ranges from $\pm 10^2$ V/m to $\pm 10^5$ V/m	±5% range max
Electrometer	Keithley	6514	2 nA 20 nA 200 nA 2 µA 20 µA 200 µA	±(0.2% RD +30 counts) ±(0.2% RD +5 counts) ±(0.2% RD +5 counts) ±(0.1% RD +10 counts) ±(0.1% RD +5 counts) ±(0.1% RD +5 counts)
Resistance meter	Static Solutions Inc.	RT-1000	10^3-10^8 Ω 10^9-10^{10} Ω 10^{11}-10^{12} Ω	±10% ±15% ±25%
Pipework thermocouples	TC Direct	1.5 mm Type T mineral insulated	–200 to 350°C	±1.5% RD
Pressure	Wika	IS-3	0-10 barg	±0.5% FS
Tank Pressure	N/A	Dial gauge	0-15 barg	Visual
Mass flow	Emerson Micro Motion	Elite CFM100M coriolis meter	0-7.5 kg/s	±3% RD*
Near-field weather station	PCE Instruments	PCE-FWS-20	0-240 km/h 10-90 % humidity	Indicator
Far-field wind sensor	Gill Instruments	Windsonic	0-60 m/s 0-359°	±3% RD ±2°
Far-field humidity sensor	Skye Instruments	SKH 2053	0-100 % -20 to 70°C	±2% ±0.05°

** Typical accuracy of 0.1 % for liquid flow at ambient temperature, estimated accuracy of 3% at cryogenic temperatures.*

3.4 Test programme

Of the 30 wall current measurements, 25 were carried out as a part of the WP3 rainout experiments, where three nozzle sizes (6 mm, 12 mm and 25.4 mm) and two pressures (1 barg and 5 barg) were used; and 5 were carried out in conjunction with the plume measurements. The six planned plume measurements experiments are shown in Table 2.

Table 2: Experimental series 4.3 test programme

Test No	Orifice Diameter	Field measurement method
4.3.1	25.4 mm	Faraday cage
4.3.2	25.4 mm	Field meter
4.3.3	12 mm	Faraday cage
4.3.4	12 mm	Field meter
4.3.5	6 mm	Faraday cage
4.3.6	6 mm	Field meter

3.5 Procedure

Over time, a portion of the LH_2 vaporises in the tank and a head of gaseous hydrogen forms, building a pressure. This subsequently increases the boiling point of the fluid in the tanker, increasing the likelihood of flashing in the pipework. Prior to each day of testing, the pressure was reduced to atmospheric pressure by releasing some of the hydrogen gas. It was then raised to the pressure in the trials. This was completed by allowing LH_2 from the bottom of the tank into the heat exchanger where vaporisation occurs. The gas was then fed into the top of the tank.

Air in the pipework with LH_2 poses significant hazards, as there is the potential to form both blockages and flammable mixtures. As such, immediately before each set of releases the pipework was purged; firstly with nitrogen, then with ambient hydrogen gas. Once the purge was complete, LH_2 could be introduced to the pipework. This operation purged the majority of the pipework, but a 1.75 m section of flexible hose located after the main release valve was not purged.

Resistance measurements were taken between the isolated pipe section and ground before some tests to enable characterisation of the charging mechanism. Recording was then initiated in the data logging software and the main release valves opened. Each experiment lasted between 2-10 minutes with the aim of achieving a steady state output from the temperature sensors within the pipework and the flow meter. Upon completion, the main release valves were closed and the vent line opened, allowing any LH_2 remaining in the pipework to vaporise and disperse safely.

4 Results

The results of the investigations into two phenomena are presented in this section; the field strength of a multi-phase hydrogen jet, and the current generated on pipework containing LH_2. Seven dedicated trials were carried out for the former, while measurements for the latter were taken in a total of 30 experiments.

As described in deliverable 3.6, the interaction between the jet formed from a cryogenic release of hydrogen and the air produces phase changes in the components of air. Of particular relevance to these investigations is the formation of a solid cone around the release point, which affected the flow of the jet in some cases. These solid deposits cyclically formed and broke off during the releases with the 6 and 12 mm nozzles. Figure 12 shows an example of a solid formation impinging the flow into two separate streams.

Figure 12: Still of jet being split in two.

4.1 Plume

A series of seven trials were carried out to measure the electrical field of a plume of cryogenic hydrogen using a field meter. These are summarised in Table 3. No significant plume measurements were obtained in five of the trials, the other two showed intermittent spikes of 100-140 V/m.

Table 3: Experimental series 4.3 summary table.

Trial No	Test No	Field meter configuration	Orifice Diameter	Pressure	Results
1	4.3.2	Free-field layout 1	6 mm	5 Bar	No significant plume measurements.
2	4.3.2	Free-field layout 1	6 mm	5 Bar	No significant plume measurements.
3	4.3.2	Free-field layout 2	6 mm	1 bar	No significant plume measurements.
4	4.3.4	Free-field layout 2	12 mm	1 bar	No significant plume measurements.
5	4.3.6	Free-field layout 2	25.4 mm	1 bar	Initial & mid-flow peaks.
6	4.3.3	Faraday cage	12 mm	1 bar	No significant plume measurements.
7	4.3.5	Faraday cage	6 mm	5 bar	Initial peak.

4.1.1 Plume Trial 5

Trial 5 was a release using the free-standing field meter setup 0.5 m from the centreline of the jet and 0.5 m from the release point. The tanker pressure was a nominal 1 barg and the 25.4 mm nozzle was used. Figure 13 shows the results. The pressure plot indicates when the release began and ended. The initial spike in field strength corresponds with the initiation of the release. Another peak in field strength corresponds with a slight peak in pressure.

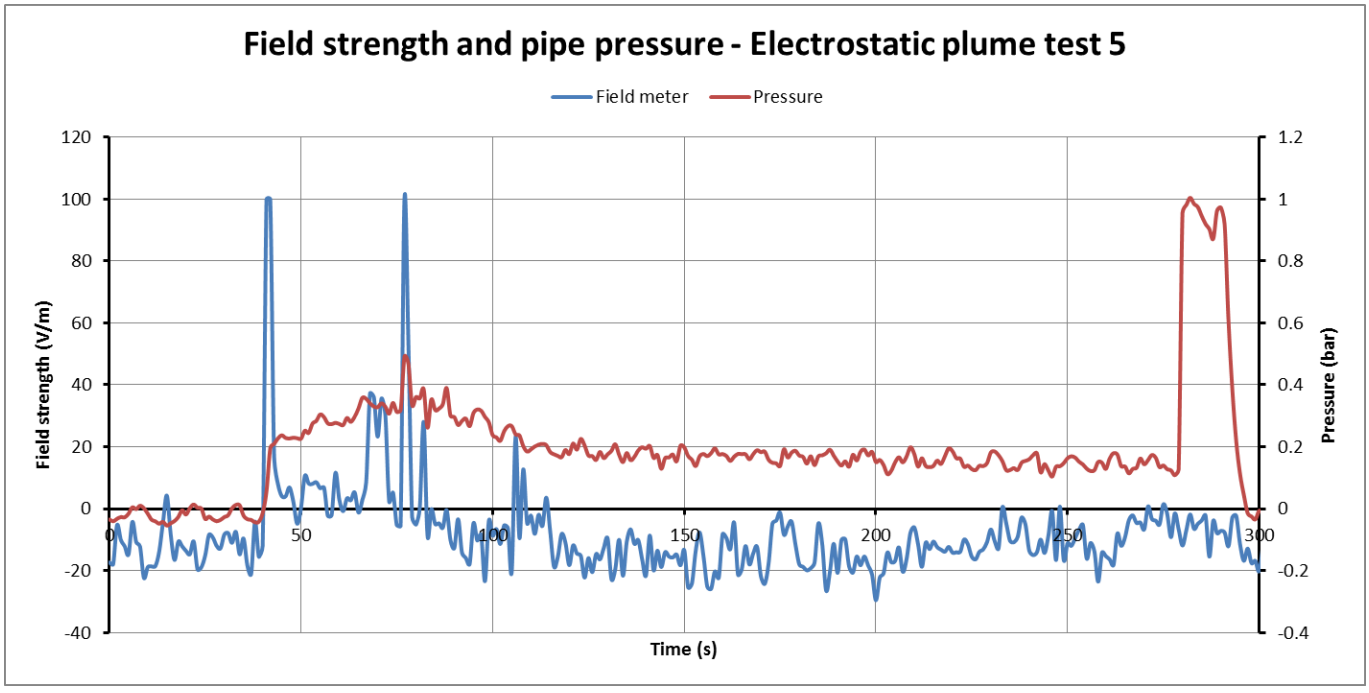

Figure 13: A graph of field strength and pipe pressure for trial 5.

4.1.2 Plume Trial 7

The field measurements in trial 7 were made using the Faraday cage. A peak was observed at the initial point, shown in Figure 14. In order to determine if the initial peak of hydrogen was charged, the release was halted and venting began multiple times throughout the trial. This is shown in the vent temperature plot of Figure 14, which indicates the mode of release. When the vent temperature is decreasing, venting is taking place; otherwise the release is through the main nozzle. In spite of multiple initiations through the main release point only one spike in field strength was observed.

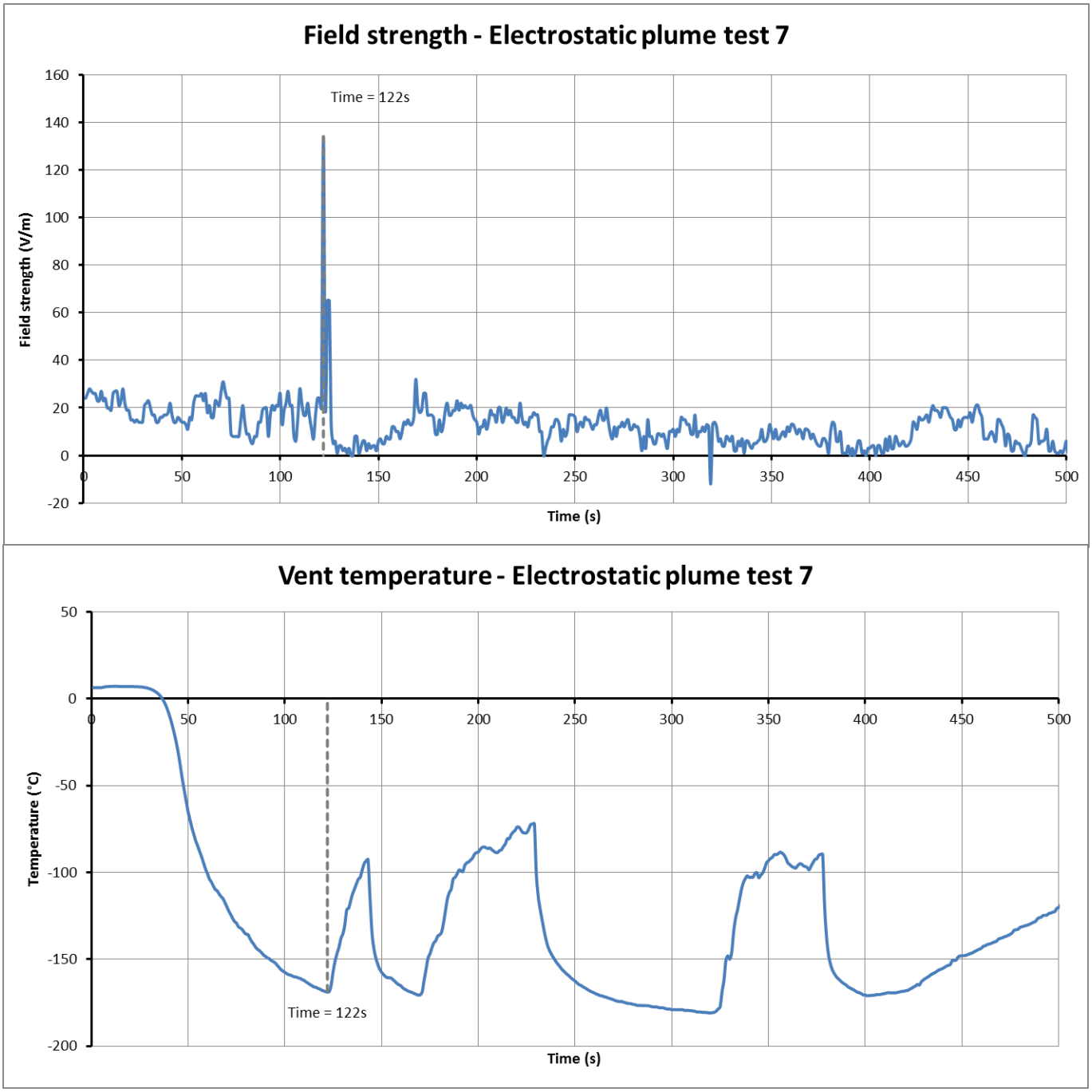

Figure 14: A graph of field strength (top), and vent temperature (bottom) for trial 7. The release mode is indicated by the vent temperature.

4.1.3 Plume Trials 1 & 2

In trials 1 and 2, no field was measured during the release. At the end, however, a slight change in field strength was observed. Figure 15 shows an example of this, with a further graph in Appendix B.

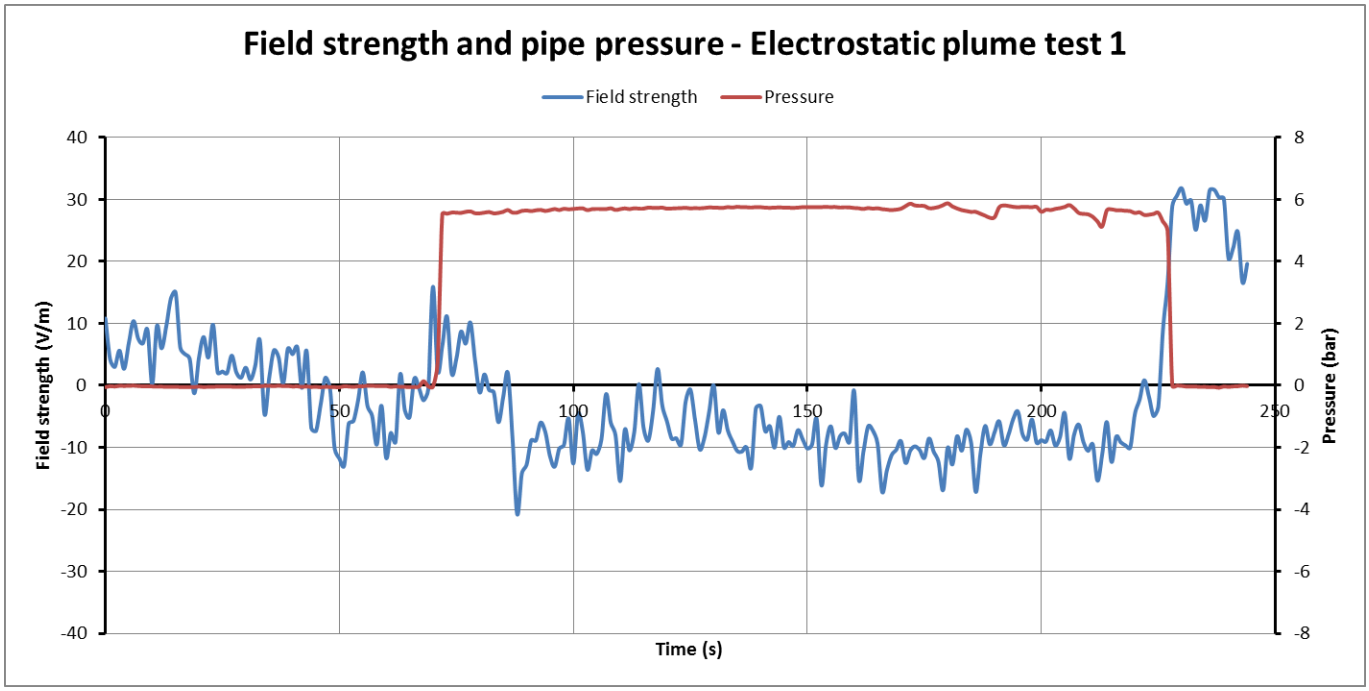

Figure 15: A graph of field strength and pipe pressure for trial 1.

4.1.4 Plume Trials 3, 4 & 6

For trials 3, 4 and 6, no clear pattern in the field meter output was observed either during or after the trials. The graphs are contained in Appendix B.

4.2 Wall current

Wall current measurements were taken on each trial in the experimental series 3.5 and trials 1 to 5 in the experimental series 4.3 – 30 trials in total. The resistance to ground of the electrically isolated section of pipework was also measured throughout each test day to analyse the results.

As with the plume measurements, a charge was not reliably generated in the pipework. When a charge was measured, the full extent is often not known due to the device over-ranging. Table 4 shows the wall current results for each of the 30 trials and the range of the electrometer. A peak value of "null" indicates that a peak or trough with a magnitude greater than the noise level was not identified. The bold entries are those that were the first in a batch of experiments completed immediately after one another. The resistance measurements were taken periodically before some tests.

Table 4: Wall current results.

Work Package	Trial No.	Orifice Size (mm)	Pressure (bar)	Wall Current peak	Range	Resistance (Ω)
3.5	**1**	**6**	**1**	**Null**	**-2 to 2 nA**	**$1.42x10^6$**
3.5	2	25.4	1	3.8 (nA)*	-2 to 2 nA	$1.06x10^7$
3.5	**3**	**25.4**	**1**	**230 (nA)***	**-200 to 200 nA**	**$1.02x10^6$**
3.5	4	12	1	Null	-200 to 200 nA	$1.06x10^7$
3.5	**5**	**6**	**1**	**240 (nA)***	**-200 to 200 nA**	**$2.48x10^6$**
3.5	6	12	1	-9.6 (nA)	-2 to 2 µA	
3.5	7	12	1	-9.6 (nA)	-2 to 2 µA	
3.5	**8**	**12**	**1**	**2.8 (µA)***	**-2 to 2 µA**	**$2.07x10^7$**
3.5	9	12	1	Null	-200 to 200 µA	$2.72x10^4$
3.5	**10**	**25.4**	**5**	**0.16 (µA)**	**-200 to 200 µA**	**$2.67x10^4$**
3.5	11	12	5	Null	-200 to 200 µA	
3.5	12	6	5	Null	-20 to 20 µA	$2.67x10^4$
3.5	13	12	5	Null	-20 to 20 µA	
3.5	14	12	5	Null	-20 to 20 µA	
3.5	15	12	5	Null	-20 to 20 µA	
3.5	**16**	**25.4**	**1**	**Null**	**-200 to 200 µA**	**$3.14x10^4$**
3.5	17	12	1	Null	-200 to 200 nA	
3.5	18	6	1	-0.27 (nA)	-200 to 200 nA	
3.5	**19**	**25.4**	**1**	**Null**	**-200 to 200 µA**	**$1.03x10^7$**
3.5	20	12	1	Null	-200 to 200 µA	
3.5	21	6	1	Null	-2 to 2 µA	
3.5	**22**	**25.4**	**4.5**	**Null**	**-200 to 200 nA**	
3.5	23	12	4.5	-0.25 (nA)	-200 to 200 nA	
3.5	24	6	4.5	Null	-200 to 200 nA	
3.5	25	25.4	4.5	-0.99 (nA)	-200 to 200 nA	$1.03x10^7$
4.3	**1**	**6**	**5.5**	**Null**	**-200 to 200 µA**	
4.3	2	6	5.5	Null	-200 to 200 µA	
4.3	**3**	**6**	**1**	**0.20 (µA)**	**-200 to 200 µA**	**$6.06x10^4$**
4.3	4	12	1	Null	-200 to 200 nA	
4.3	5	25.4	1	-0.35 (nA)	-200 to 200 nA	

** Result was above the selected range on the electrometer.*

Experiments 2, 3, 5, and 8 all showed similar behaviour in that part way through a release, the wall current sharply rose to a value above the maximum of the range on the electrometer. This is demonstrated in Figure 16, which show the wall current, temperature and mass flow rate for WP3 trial 8. The temperature and mass flow rate graphs indicate the phase of the fluid. The temperature sensor is located before the electrically isolated pipe and the mass flow meter after. Some trials did contain measurements within the range of the instrument. These typically occurred when the resistance measurements indicated a low resistance to earth from the electrically insulated pipe. Figure 17 show results from WP3 trial 10.

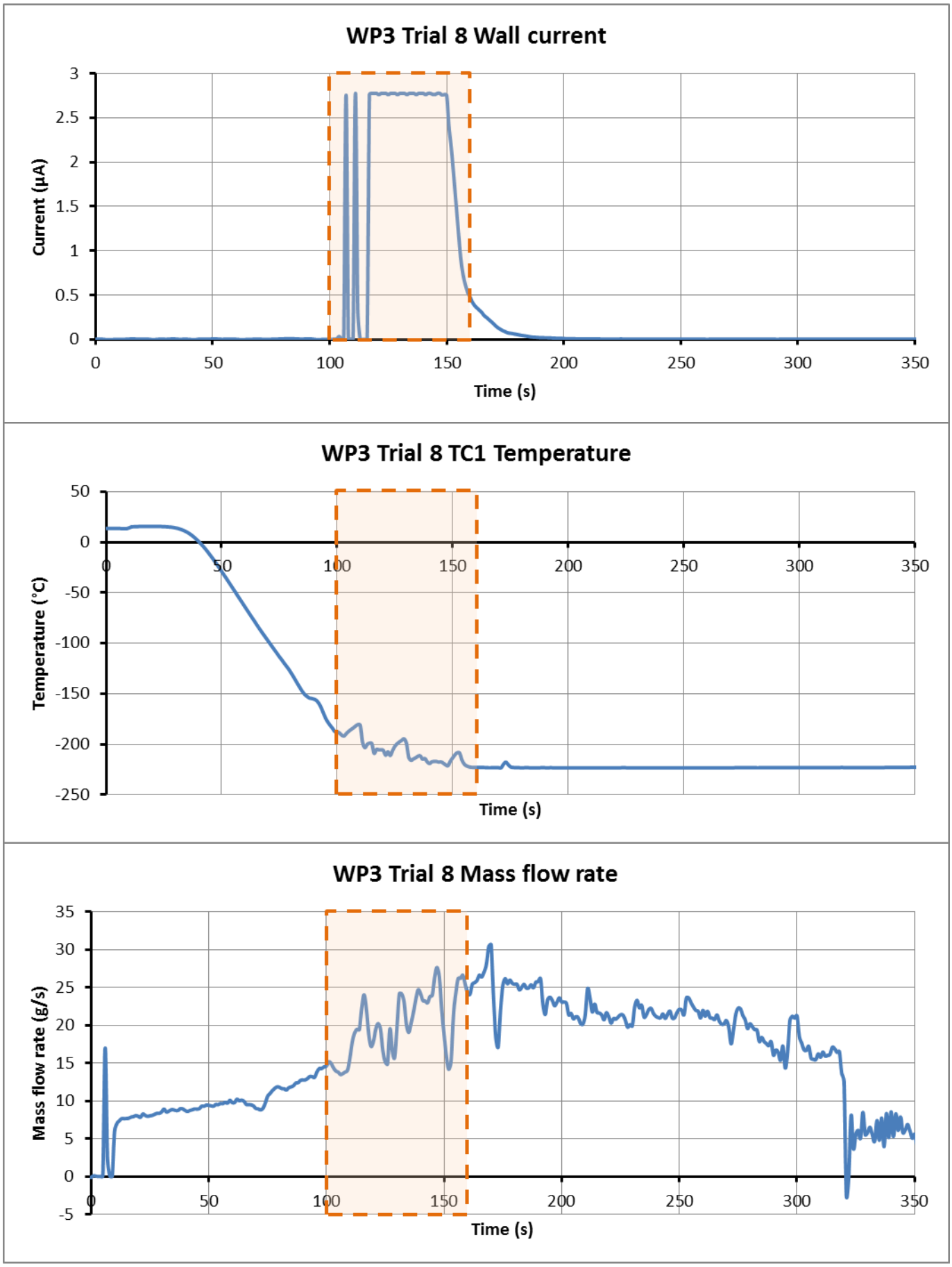

Figure 16: Wall current, temperature and mass flow rate results for WP3 trial 8.

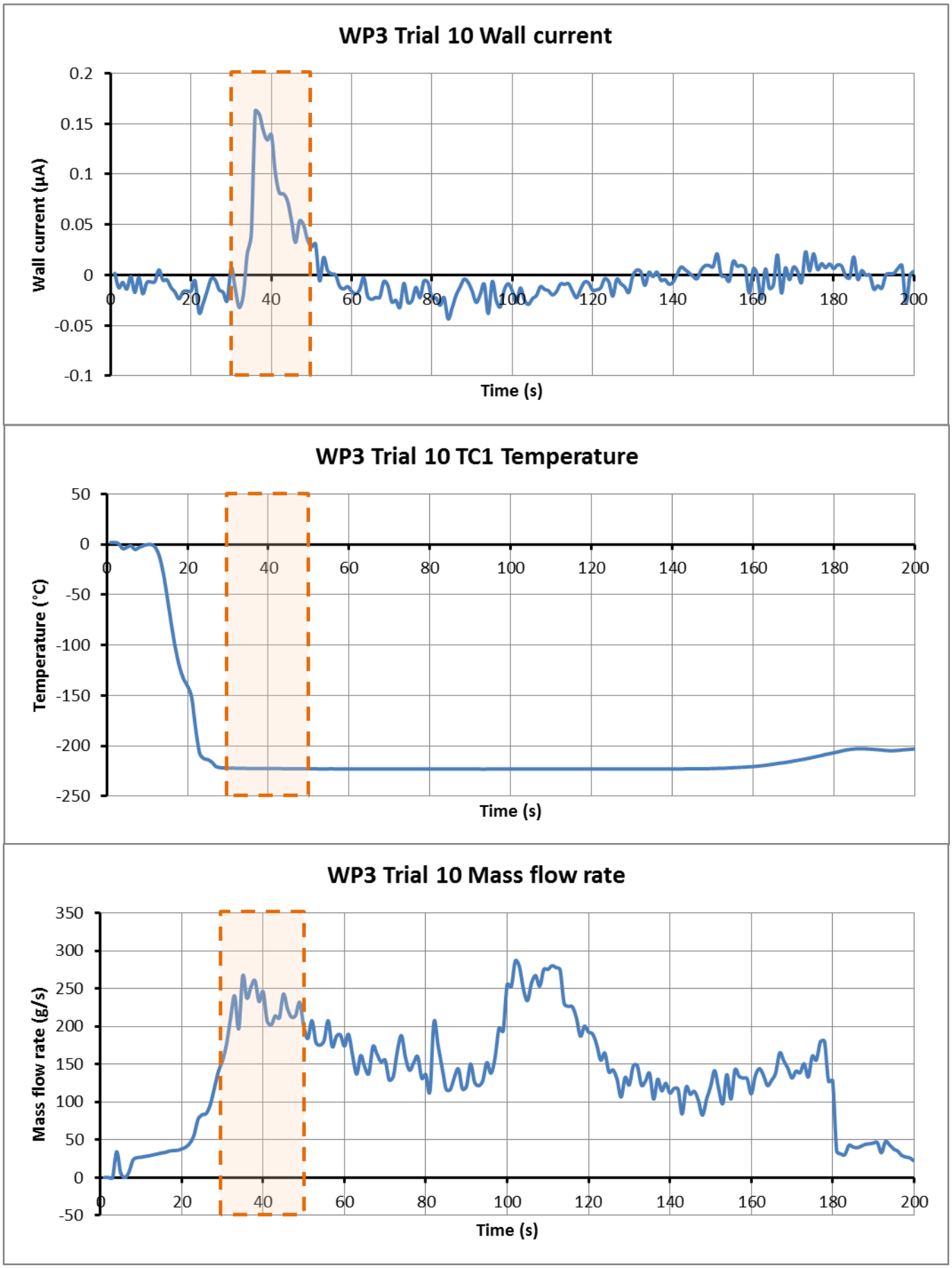

Figure 17: Wall current, temperature and mass flow rate results for WP3 trial 10.

4.3 Ice formation

A factor that affected the results was the build-up of frost on the electrically isolated pipework section. Figure 18 shows this section of pipework following a trial. Once the frost had developed the resistance measurements were orders of magnitudes lower (typically around 10^4 Ω rather than 10^7), which would limit the amount of current generation by causing a larger leakage rate.

Figure 18: Frost around an electrically isolated joint.

5 Discussion

Two phenomena were investigated as a part of this experimental series: the propensity for a plume created by a cryogenic release of LH_2 to have an electrical charge, and the capacity for LH_2 in pipework to induce a charge on the pipework. The results can be used to infer qualities of the LH_2.

5.1 Plume measurements

With only two of the seven trials showing identifiable fields in the plume, it is clear that cryogenic hydrogen releases at relatively low pressures (maximum of 5 barg) did not reliably generate an electric field under the conditions of the experiments. In both of the trials that obtained positive results, a spike of 100-140 V/m was recorded as the flow was first initiated. Since the initial spikes correlated with the opening of the release valve it is unlikely that hydrogen generated the charge, but rather the air in the final 1.75 m section of pipework (which remained open to the air between tests and was not purged) being ejected in a turbulent manner. This is further supported by the results of trial 7, which contains multiple initiations of the release as the operation was changed from venting to a main release three times, with only the initial one showing the spike in field strength. During the venting stage of this trial, cryogenic hydrogen was still present in the pipework and would be expanding out of the main release point as it warmed, causing a slightly positive pressure and meaning air entrainment back into the pipework was unlikely, therefore no charge was generated upon the re-initiation of the release.

The lack of this phenomenon in the other trials could be due to either no field being generated due to insufficient levels of air or turbulence in the release, or the measurement device being too far to register the small and transient charge. It is worth noting that positive results were only obtained with the field meter close to the release point.

The other result of interest in the plume measurements was the secondary spike and corresponding pressure increase in trial 5. While not confirmed, this secondary pike and rise in pressure could have been caused by a phase change in the air around the nozzle creating a cone of solid air impinging the flow and subsequently breaking off and registering a charge with the field meter.

Test 4.3.1, which was a full bore (25.4 mm) release through the Faraday cage was not carried out due to concerns of the proximity of the cage and field meter to the resulting plume.

From these plume measurements, it is clear that while a transient field can be measured, a charged plume forming from an established cryogenic jet is unlikely for the initial conditions of these experiments.

5.2 Wall current

The balance between the charge generation from the action of the process fluid on the pipework and the leakage to earth is the wall current, which is heavily dependent on the resistance to earth of the pipework. This makes the interpretation of the results difficult as the resistance changes dynamically through the trials due to the formation of frost. The resistance measurements are taken between trials and therefore only give an indication of the true value. For the trials with an indicated value in the order of 10^4 Ω it is possible that charge generation is occurring, but at a rate insufficient to overcome the leakage to

earth. The reduction in resistance caused by the frost means that the initial trial in a batch produces favourable conditions for wall current measurements.

It is postulated that the primary mode of charge generation during these experiments is the kinetic energy transferred from a roiling two-phase flow to the surrounding pipework, which is supported in previous work by Cassutt *et al* [5] whereby charge generation was observed as most serious during two-phase flow. This is supported for low pressure (maximum of 5 barg) releases by the correlation of the charge generation and the phase of the fluid as indicated by TC1, which is located at the inlet to the section of electrically insulated pipework; and the mass flow meter, which is located downstream. The temperature graphs contain three distinct regions: the initial smooth reduction in temperature, a single phase gas flow; an oscillatory reduction in temperature, a two-phase flow; and a final steady state, a full liquid flow. The charge generation consistently falls within the two-phase region of the graph. Similarly, the mass flow meter is unable to resolve two-phase flow, resulting in an unstable output. This unstable region correlates well with the charge generation as well. For the high pressure releases, the temperature of TC1 does not show the oscillatory period, but the charge generation does correlate with the initiation of the two-phase flow as indicated by the mass flow meter. This is illustrated in the results for trial 10.

An extension of this mode of charge generation is that any initial condition that encourages or extends the two-phase flow will also cause more generation. This includes the initial state of the pipework being relatively warm as more heat transfer into the process fluid will result in more vaporisation; a further reason that the initial trial in a batch seems to encourage charge generation. Other initial conditions that affect the phase of the fluid in the pipe are the tanker pressure and the release nozzle size. The 5 barg releases have a higher volumetric flow rate that therefore decreases the time it takes for the pipework to cool, reducing the period of two-phase flow. The 25.4 mm nozzle is similar in that a predominantly liquid flow is developed quickly, even during the 1 barg releases. Conversely, the choked flow of the 6 mm nozzle produces a significant back pressure, extending the latency of the hydrogen in the pipe, potentially resulting in a more gaseous flow rather than a turbulent two-phase flow, thereby reducing the charge build-up.

From these trials it is evident that the flow of LH_2 in pipes can cause electrostatic charges and that certain conditions encourage it. The applications of these findings revolve around either designing LH_2 pipework so that the development of two-phase flows are limited (through vacuum insulation, for instance) or ensuring that the pipework contains no electrically isolated sections.

6 Conclusion

The PRESLHY project experimental programme has been designed to provide insight and data on poorly understood and high risk scenarios. This includes the propensity for LH_2 to generate a static charge large enough to cause ignition of a hydrogen cloud. The series of experiments summarised in this report investigate two distinct charging modes that could lead to such an electrostatic discharge: a charge developing within a multiphase hydrogen jet, and a charge developing on a section of pipework containing LH_2. A series of seven plume measurement experiments were completed and wall current measurements were made on a total of 30 LH_2 releases.

While occasional spikes in field strength were observed on the multiphase hydrogen jet that forms during a release of LH_2, the plume itself did not become charged. The spikes have been attributed to the air, either in the form of air in the pipework being ejected or complex phase changes around the release point causing solids to flow downstream. Different initial conditions could result in a higher degree of field strength in the plume.

Across the 30 trials in which wall current measurements were taken, it is evidenced that LH_2 flowing in electrically insulated pipework can generate a charge. This occurs from the action of a turbulent two-phase flow on the surrounding pipework. Initial conditions that encourage a turbulent two-phase flow also encourage charge generation in the pipework. For ground-based applications, continuity between the pipework and earth is important to avoid charge build-up.

7 References

[1] Lyons, K., Coldrick, S. (2020) Summary of experiment series E3.5 (Rainout) results. Deliverable 3.6, Pre-normative REsearch for Safe use of Liquid HYdrogen (PRESLHY)

[2] Lyons, K., Proust, C., Cirrone, D., Hooker, P., Kuznetsov, M., Coldrick, S. (2020) Theory and analysis of ignition with specific conditions related to cryogenic hydrogen. Deliverable 4.1, Pre-normative REsearch for Safe use of Liquid HYdrogen (PRESLHY)

[3] Cross, J.A., Hilger, A. (1987) Electrostatics – Principles, problems and applications, ISBN 0-85274-589-3, Bristol.

[4] Personal communication from G. Necker, 28/02/19.

[5] Cassutt, L., Biron, D., Vonnegut, B. (1961) Electrostatic hazards associated with the transfer and storage of liquid hydrogen. Advances in Cryogenic Engineering: Proceedings of the 1961 Cryogenic Engineering Conference, University of Michigan Ann Arbor, pp 327-335.

8 Appendix A – Data sheet

A series of seven unignited liquid hydrogen (LH_2) trials were conducted to investigate the propensity of LH_2 to generate and hold an electrostatic charge. This was done by releasing LH_2 into the path of a field meter. Some trials included a Faraday pail. Instrumentation measuring the outflow properties and ambient conditions, such as humidity, enable a more thorough analysis of the plume measurement results. These dedicated trials were supplemented with wall current measurements taken on 25 other trials that were carried out in separate work packages in the PRESLHY project. Details of the experimental setup, instrumentation, data acquisition and results formats are described with the aim of providing the necessary context to fully interpret the results.

8.1 Experimental Set-Up

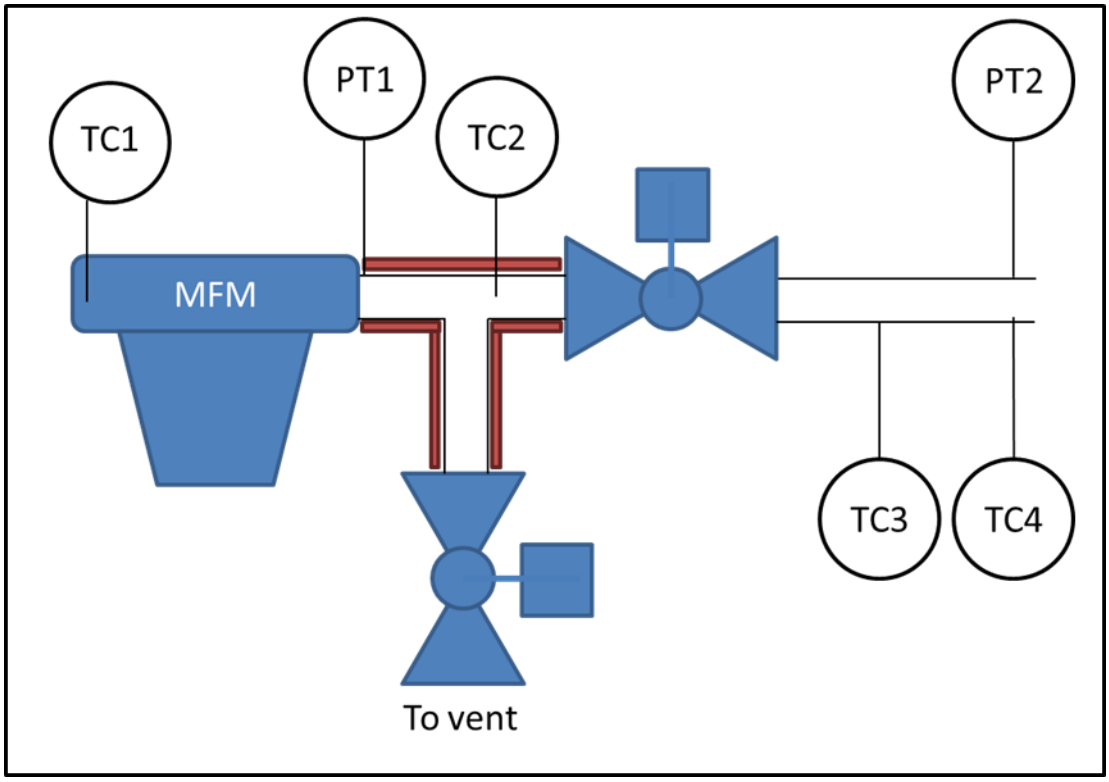

Figure A1: Sketch of the LH_2 release facility with instrumentation.

Table A1: Sensor positions on the release pipework.

Name	Description	Distance to release point (m)
TC1	In-flow thermocouple	3.25
WS	Weather station	2.75
MFM	Mass flow meter	2.55
TC2	In-flow thermocouple	2.35
PT1	Pipework pressure transducer	2.35

PT2	Pipework pressure transducer	0.08
TC3	In-flow thermocouple	0.08
TC4	Pipework wall thermocouple	0.02

Table A2: Dimensions of 25.4 mm nominal bore pipe sections.

Description	Length (m)	Thermal conductivity (W/m.K)*
Vacuum insulated hose	20	2.5 W/m
Electrically isolated pipe	0.5	0.021
Mass flow meter	0.4	n/a
Valve section	0.6	13-17
Flexible hose	1.75	0.034

**Typical values for the insulation materials are given, taken from the datasheets of the manufacturers. The vacuum insulated hose had units of W/m.*

Table A3: Locations of weather stations.

Weather station	Model	Distance (m)	Height (m)	Angle from release point	Angle from North
Local	PCE	2.75	1.5	180°	255°
Far-field	Windsonic & Skye	20	3	-15°	60°

Note the release pointed at approximately 75° from North.

8.2 Data Acquisition Systems

Table A4: Channel settings for the primary acquisitions system

Instrument	Column header	Units	Description
Cold junction thermocouple	Cold_junction	°C	Cold junction temperature
Cold junction thermocouple	Cold_junction_error	µV	Cold junction thermovoltage
Isolated pipe current	EV1_Streaming_current	nA*	Current
Field meter	Field meter	V/m	Field strength of the plume
Flow meter	MFM1_Mass_Flow_Rate	g/s	Mass flow through meter

Flow meter	MFM2_Drive_Gain	%	Flow meter drive gain
Pressure transducer	PT1_Pipe_Pressure	barg	Pressure at outlet nozzle
Pressure transducer	PT2_Nozzle_Pressure	barg	Pressure downstream from flowmeter
Weather station	Relative_Humidity	%	Weather station at pad edge
Pipework thermocouples	TCX_abcd	µV	Thermovoltage from pipework thermocouple X
Pipework thermocouples	TCX_abcdC	°C	Temperature from pipework thermocouple X
Weather station	Wind_Direction	°	Wind direction from N
Weather station	Wind_Speed	m/s	Wind speed at 3 m

**Units changed to µA for some tests due to over-ranging.*

9 Appendix B – Results

9.1 Plume measurement results

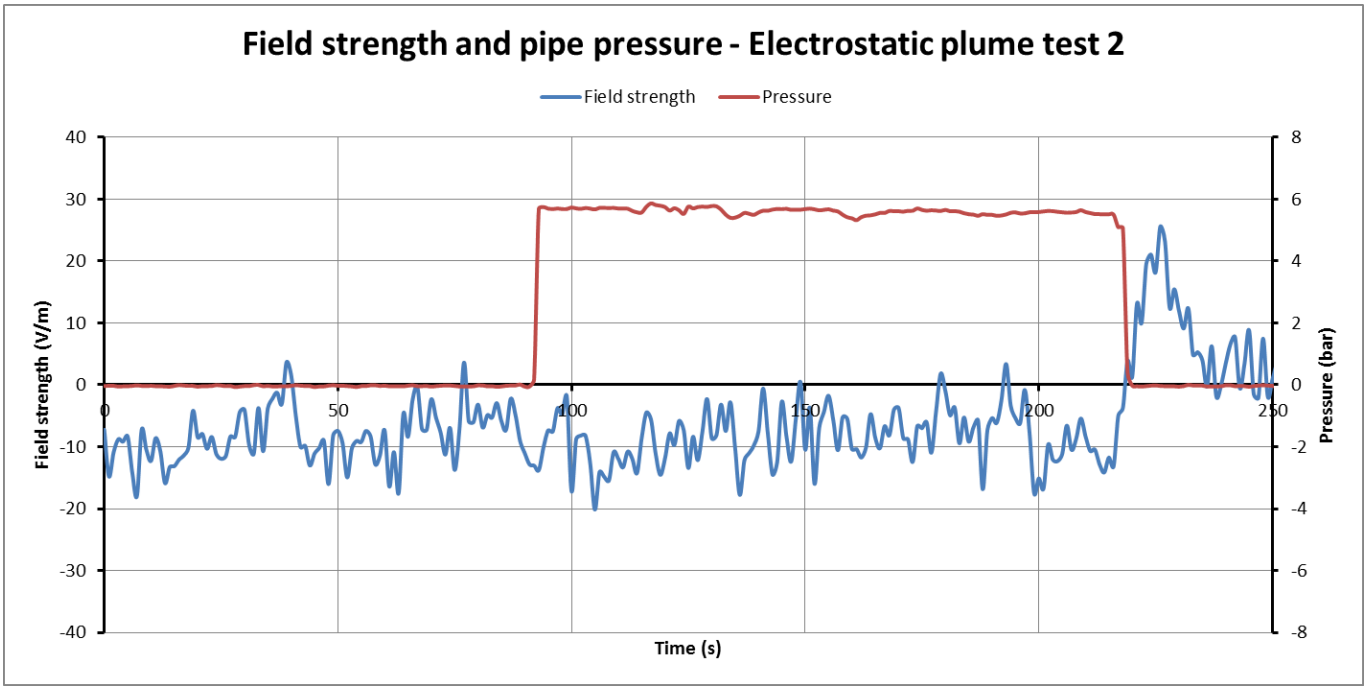

Figure B1: Plume field strength and nozzle pressure.

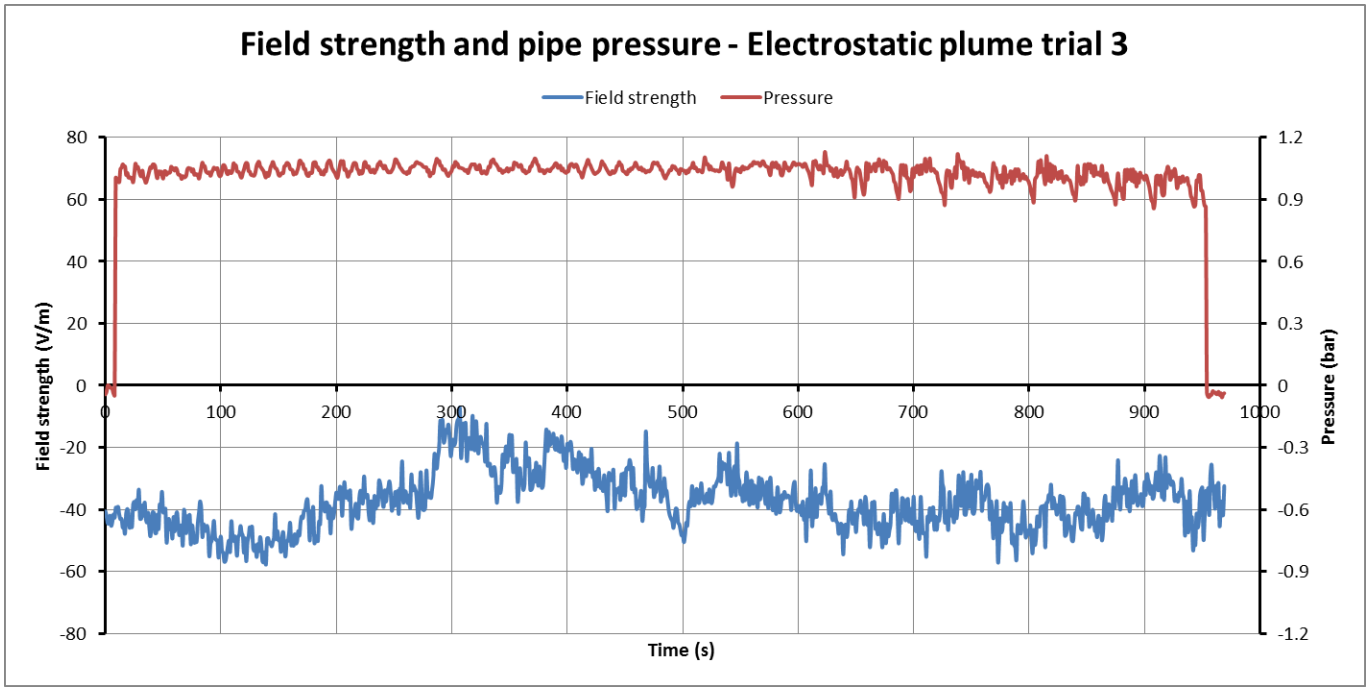

Figure B2: Plume field strength and nozzle pressure.

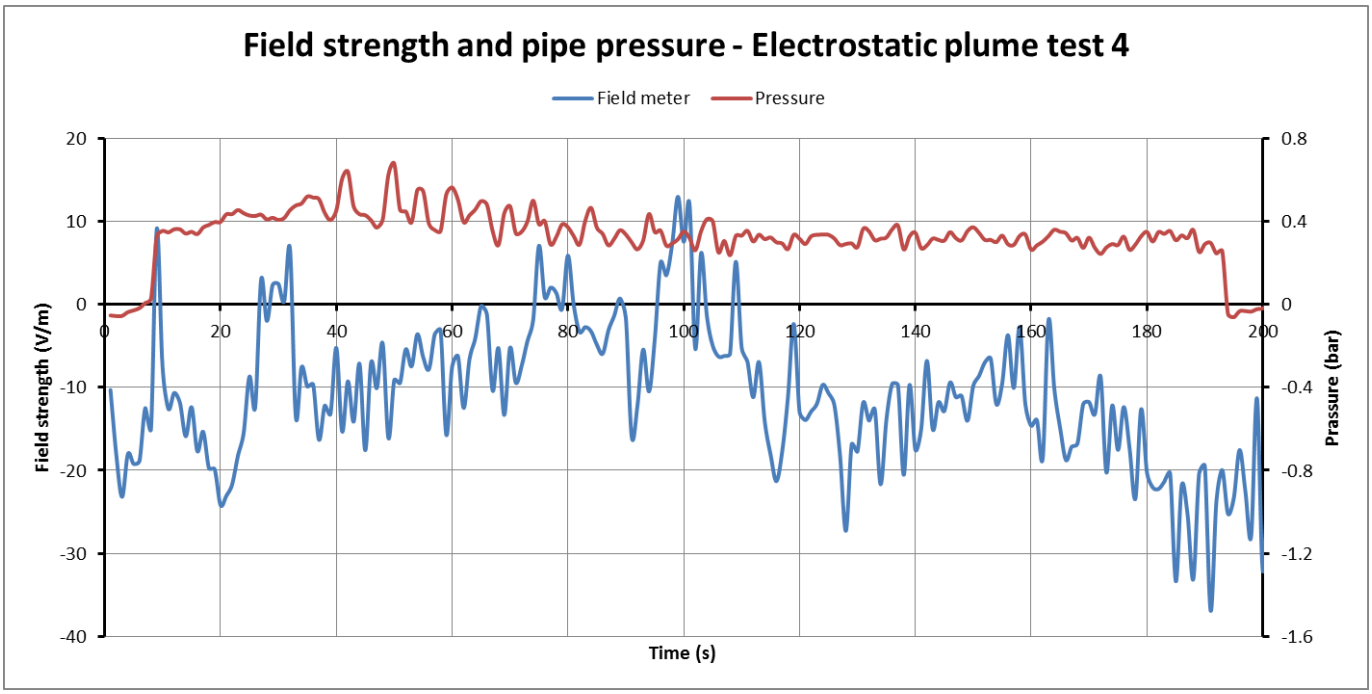

Figure B3: Plume field strength and nozzle pressure.